SPECTROSCOPIC ANALYSIS OF THE ZINC ION INTERACTION WITH HORSERADISH PEROXIDASE**

Najmeh Hadizadeh Shirazi*, Mohammad Reza Rajabi

Department of Biology, Roudehen Branch, Islamic Azad University, Roudehen, Iran;
e-mail: na.hadizadeh@iau.ac.ir

The purpose of the current study was to evaluate the interaction between zinc ions and horseradish peroxidase (HRP) by ultraviolet-visible, fluorescence, circular dichroism, and FTIR spectroscopies. HRP conformation analysis revealed a noticeable decrease in α-helix from 47% for the free enzyme to 17% for HRP–Zn^{2+} and a reduction in tertiary structures of the enzyme through a Zn^{2+} interaction. Moreover, the fluorescence intensity of HRP was decreased significantly by Zn^{2+}. The linear relationship of HRP emission data and inhibitor concentration indicated that the extinction process is linear and occurs uniformly with increasing Zn^{2+} concentration. The values of K_q for the zinc and HRP interaction were in the order of 10^{11} l/mol, which means that HRP fluorescence was quenched by Zn^{2+} through a static quenching mechanism.

Keywords: *horseradish peroxidase, zinc ion, spectroscopy, structure.*

СПЕКТРОСКОПИЧЕСКИЙ АНАЛИЗ ВЗАИМОДЕЙСТВИЯ ИОНОВ ЦИНКА С ПЕРОКСИДАЗОЙ ХРЕНА

N. H. Shirazi*, M. R. Rajabi

УДК 543.42:(546.47+577.158.52)

Рудехенский филиал Исламского университета Азад, Рудехен, Иран;
e-mail: na.hadizadeh@iau.ac.ir

(Поступила 6 июня 2022)

С помощью УФ-видимой, флуоресцентной, ИК-Фурье-спектроскопии и кругового дихроизма проанализировано взаимодействие ионов цинка и пероксидазы хрена (HRP). Анализ конформации HRP выявил заметное уменьшение α-спирали с 47% для свободного фермента до 17% для HRP–Zn^{2+} и уменьшение третичных структур фермента за счет взаимодействия с Zn^{2+}. Интенсивность флуоресценции HRP значительно снижается вследствие наличия Zn^{2+}. Линейная зависимость интенсивности излучения HRP от концентрации ингибитора показала, что процесс вымирания является линейным и происходит равномерно с увеличением концентрации Zn^{2+}. Для взаимодействия цинка и HRP $K_q \approx 10^{11}$ л/моль. Это означает, что флуоресценция HRP подавляется Zn^{2+} с помощью механизма статического тушения.

Ключевые слова: *пероксидаза хрена, ион цинка, спектроскопия, структура.*

Introduction. Most heavy metals have toxic effects on cellular activity, even at low concentrations. As they enter the food chain through the feeding and breathing of living organisms, their environmental pollution is a major global problem. Although heavy metals such as zinc (Zn^{2+}) are vital for the cellular activity of living organisms, their ecological contamination does not cause much concern. Some significant sources of Zn^{2+} contamination in soil are industrial products such as wood preservatives, factory waste and slags, mine tailings, and coal ash [1]. Many investigations indicated the phytotoxic effect of Zn^{2+} on plants at high concentrations. Moreover, it accumulates in the roots of plants and poses health risks to consumers [2]. The

**Full text is published in JAS V. 90, No. 1 (http://springer.com/journal/10812) and in electronic version of ZhPS V. 90, No. 1 (http://www.elibrary.ru/title_about.asp?id=7318; sales@elibrary.ru).

cytotoxic doses of Zn^{2+} play an essential role in disturbing many cellular events such as apoptosis and cellular respiration [3]. Increased intracellular free radicals and the impaired permeability of mitochondrial membranes and electron transfer chain along with the subsequent inhibition of oxidoreductase enzyme functions such as superoxide dismutase and peroxidase are among the effects of high concentrations of Zn^{2+} [4].

Peroxidases participate in biochemical processes such as thyroid hormone biosynthesis, conjunctions of cell-wall constituents, cellular detoxification, and inflammatory disease pathogenesis in plants and animals [5]. Peroxidase inhibition has a significant role in cytotoxicity, apoptosis, aging, and animal or plant diseases. Cellular ROS content has been constantly controlled by several enzymatic antioxidant defense systems consisting of peroxidase [6]. Horseradish peroxidase (HRP) has an important place in research, as does the production of enzyme-based biotechnology products, such as biosensors, owing to their suitable size, high stability, and, of course, easy access to other peroxidases [7]. Moreover, according to the multiple sequence alignment, there are highly conserved catalytic residues between different heme-containing peroxidases [8]. Hence, HRP has been considered a research model enzyme for peroxidases [9, 10].

Although peroxidase is known as a thermostable enzyme, its activity is strongly affected by the ionic strength of its surroundings [11]. Pandey and coworkers reported that high doses of Fe^{3+} and Zn^{2+} inhibit peroxidase activity [12]. Similar results have been reported for the toxic effect of other heavy metals such as Hg^{2+}, Ni^{2+}, Al^{3+}, and Pb^{2+} on peroxidase activity [13, 14]. Also, HRP inactivation occurs at pH extremes or when excess H_2O_2 is present [15].

HRP C, an HRP isoform, is an α-helical polypeptide that consists of 308 amino acids, a Fe^{3+}, and two Ca^{2+} metal centers [11]. The prosthetic group of HRP is a Fe^{3+}-included porphyrin called heme. Behera et al. indicated that Leu80His mutation, located in the distal of the heme pocket, facilitates the formation of redox intermediates and increases the HRP activity [16]. In contrast, oxidative stress or phenolic groups inhibit the enzyme by reducing the heme group's flexibility [17]. Therefore, heme group destruction and instability have a critical role in HRP inactivation [17].

Our previous study indicated that the excess amount of Zn^{2+} inhibits the catalytic activity, and changes the thermal inactivation pattern of HRP [18]. Owing to the significant role of HRP structure and its heme group in enzyme activity and thermal stability and the importance of peroxidases in industry, it is necessary to analyze the peroxidase structure in the presence of Zn^{2+}. For this purpose, the secondary and tertiary structures of HRP in the presence of different concentrations of zinc ion have been monitored using UV-Visible spectroscopy, circular dichroism, and Fourier transform infrared (FTIR). Moreover, the photo biochemistry properties of the enzyme have been studied by fluorescence spectroscopy.

Materials and methods. The lyophilized powder of HRP was procured from Sigma Aldrich Co. and dissolved in 100 mM potassium phosphate buffer (pH 6) for the experimental studies. The enzyme purification index (Rz value) of HRP was determined by calculating the heme (at 403 nm) to the protein (at 280 nm) absorbance ratio [19]. The Rz value for HRP was more than 2.0. All solutions were prepared with redistilled, ion-free water, and all assays were performed in triplicate. All other purchased chemicals were of analytical grade. The zinc chloride ($ZnCl_2$) was purchased from Merck (Germany). The appropriate amount of $ZnCl_2$ was dissolved in redistilled water to prepare 0–500 μM inhibitor solutions.

The UV-Visible spectra of HRP in the presence of 0–500 μM $ZnCl_2$ within the range 220–320 nm was obtained at room temperature while maintaining an HRP concentration of 0.1 mg/mL in 1.0-cm quartz cells. The UV-Visible absorption data were recorded by a Shimadzu spectrophotometer (Japan). The HRP solutions were incubated for 5 min at 4ºC before all spectroscopic studies to achieve equilibrium.

The circular dichroism (CD) spectra have been obtained with JASCO J-715 (Japan) at 190–230 nm (far-UV CD spectra) and 230–320 nm (near-UV CD) at room temperature. The enzyme concentration was kept constant at 0.2 mg/ml, and the spectra were recorded with the 0.1- and 1.0-cm quartz cuvettes for far- and near-UV CD spectra, respectively. Far-UV CD data were expressed as molar ellipticity, $[\theta]$ $(\text{deg} \cdot \text{cm}^2 \cdot \text{dmol}^{-1})$, assuming the mean amino acid residual weight (MRW) of HRP to be 110 [20]. The molar ellipticity was determined as: $[\theta] = (\theta \times 100\ \text{MRW})/(Cl)$, where C and l are the protein concentrations in mg/mL and the light path length in centimeters, respectively. To enhance the signal-to-noise ratio, the spectra have been smoothed using JASCO J-715 software, including the fast Fourier-transform noise reduction routine [19].

A Nicolet 8700 FTIR spectrometer and ATR accessory were used to record FTIR spectral data within the range 4000–500 cm^{-1} [3]. Each spectrum has been prepared from an average of 32 scans with a resolution of 2 cm^{-1}, and the background and water spectra were initially prepared and automatically reduced from the spectra. An HRP concentration of 10 mg/mL was used for all experiments, and the samples were pre-

incubated for 1 h to achieve equilibrium. The data processing and second derivatives of spectra deconvolution were done by spectrometer software and Origin Pro.

The photo biochemistry properties of HRP were obtained using a PerkinElmer fluorescence spectrometer at various concentrations of $ZnCl_2$ and a constant enzyme concentration of 1 mg/mL. The enzyme was excited at 295 nm, and the collected emission spectra were within the range 300–400 nm with a 4-mL quartz cuvette at room temperature and scan rate of 500 nm/s. HRP–$ZnCl_2$ solutions were allowed to settle for 2 min to achieve equilibrium.

The Stern–Volmer equation was used to evaluate the fluorescence-quenching mechanism of HRP [21]:

$$F_0 / F = 1 + K_{SV}[Q] = 1 + K_q \tau_0 [Q],$$

where F_0/F is the fluorescence intensities ratio of HRP and HRP–$ZnCl_2$ solutions, and K_{SV}, K_q, and $[Q]$ are the Stern–Volmer quenching constant, the quenching rate constant of HRP, and zinc ion concentration, respectively. The average lifetime of the HRP fluorescence in the absence of zinc ion (τ_0) is 10^{-8} s. Assuming that the quencher molecules are independently attached to the binding site on the macromolecule, the fluorescence data have been further examined using modified Stern–Volmer equations [22]:

$$F_0 / \Delta F = [1 / f_a K_a][1 / [Q]] + 1 / f_a,$$

$$\log \frac{F_0 - F}{F} = \log K + n \log [Q],$$

where f_a is the accessible fluorophore to the quencher; K_a is the Stern–Volmer quenching constant of f_a; K is the binding constant, and n is the number of binding sites.

Results and discussion. UV-Vis absorption measurement is one of the most applicable methods used in structural studies of ligand–protein complexes [23]. Our previous studies showed that the enzyme is inhibited in the presence of 100 μM Zn^{2+} and that the behavior of the enzyme changes from mono-phase to biphase inactivation at high zinc concentrations [19]. Various studies have shown that the LD50 values of free zinc ions range from 40 to 350 μM for different cell lines, such as cardiac myocytes, human colorectal adenocarcinoma cells, human epithelial cervical adenocarcinoma, and cortical neurons. Owing to the variation of the toxic concentration of zinc ions, the range 0–500 μM was considered in this research [24]. A strong absorption peak due to the aromatic residue absorption has been observed at 280 nm (Fig. 1). Despite the slight enhancement in HRP absorbance intensity at higher concentrations of Zn^{2+}, the interaction of HRP with Zn^{2+} resulted in a minor redshift of the spectrum, which is most likely due to the complex of HRP with Zn^{2+} [21].

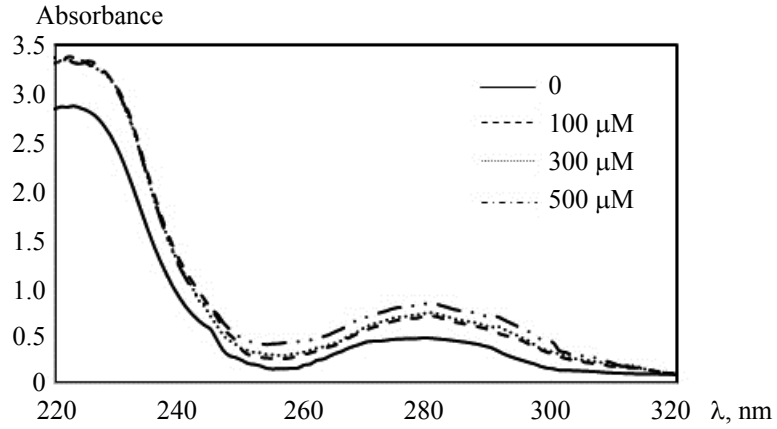

Fig. 1. UV-absorbance spectra of HRP in the presence of 0–500 μM Zn^{2+} at pH 6.0 and room temperature.

The far- and near-UV CD spectra were obtained to study the influence of Zn^{2+} on the secondary and tertiary structure of HRP, respectively (Fig. 2). The secondary structure of HRP decreased slightly owing to the interaction between Zn^{2+} and HRP (Fig. 2a). The spectrum pattern corresponds to the α-helix structure with two negative minima at 208 and 222 nm. The far-UV CD spectra deconvolution indicated that the free form of HRP has 39.9% α-helix, which is consistent with other studies [25]. However, helicity decreased to 28.6, 27.5, and 26.7% after gradually adding 100, 300, and 500 μM Zn^{2+}, respectively. The decrease in the value of ellipticity reflects the alterations in the secondary structure of HRP upon Zn^{2+} binding [26]. The ππ* elec-

tronic excitations of aromatic residues and their sensitivity to the symmetry and nature of local surroundings are responsible for the signals obtained in the near-UV region CD data [27]. Near UV-CD spectra analysis revealed that free HRP had a negative minimum at 288 nm owing to the tryptophan absorbance [28] and that its absorbance intensity was reduced in the HRP–Zn^{2+} complex (Fig. 2b). These results show that the third structure is significantly more affected by the interaction with Zn^{2+} than the secondary structure (Fig. 2b). As far- and near-UV-CD spectra provide general information about HRP configurations, the secondary and tertiary structures of the enzyme were investigated in detail by FTIR and fluorescence spectroscopy techniques, respectively.

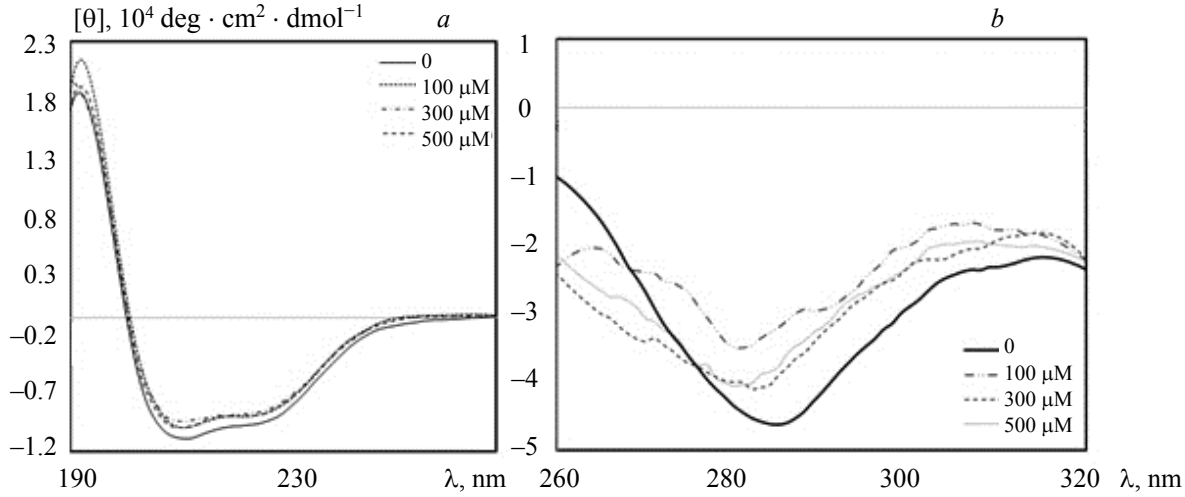

Fig. 2. Circular dichroism spectra of HRP at (a) a far UV-CD region and (b) a near UV-CD region in the presence of 0–500 μM Zn^{2+} at pH 6 and room temperature.

The FTIR spectrometer provides valuable information about molecular bonds such as N–H, O–H, and C–H stretches and their vibrational absorption levels in proteins. Analyzing the FTIR data for the chemical bond stretches of proteins provides essential information about the amide bands (amide I, II, III, IV, V, and VI bands), the peptide linkages of the protein backbone, and the local secondary structure. As the amide I band has a high sensitivity to the hydrogen bonds and carbonyl stretching vibrations of the peptide bonds at wavenumbers 1716–1574 cm^{-1}, it is used frequently for the α-helix and β-sheet content of protein structure determination [29]. In contrast, the sensitivity of the amide II band (at 1574–1483 cm^{-1}) is derived mainly from in-plane N–H stretching vibration and shows much less protein conformational sensitivity than the amide I band [30]. The FTIR results indicated that the presence of Zn^{2+} decreases the intensity of HRP in the amide I and amide II bands, suggesting the reduction of the α-helix content in the secondary enzyme structure at relatively high Zn^{2+} concentrations (Fig. 3a) [29]. HRP secondary structure content was estimated by considering amide I second derivatives decomposition and determining the centers of Gaussian contours

TABLE 1. Decomposition of Amide I Bands of HRP in the Presence of 0–500 μM Zn^{2+}

Compound	Band assignment in water, cm^{-1}	Area of each Gaussian contour, %			
		0 μM Zn	100 μM Zn	300 μM Zn	500 μM Zn
Helix	1648–1657 1663	47	30	25	17
β-sheet	1626–1640 1674–1695 1612–1640	21	24	25	13
Turn	1655–1675 1680–1696	4	4	3	4
Random coil	1640–1651	28	42	47	66

N o t e. Secondary structure has been calculated from the individual Gaussian contours fitted to the amide I IR spectra.

(Figs. 3b,c). The area of each Gaussian contour represents the contribution of the definite type of the secondary structure [30]. The binding interaction of Zn^{2+} with HRP resulted in a significant reduction in the α-helix from 47% for free HRP to 17% for the HRP–Zn^{2+} complex and a slight increase in the β-sheet from 21% free HRP to 13% in the presence of 500 μM Zn^{2+} (Table 1).

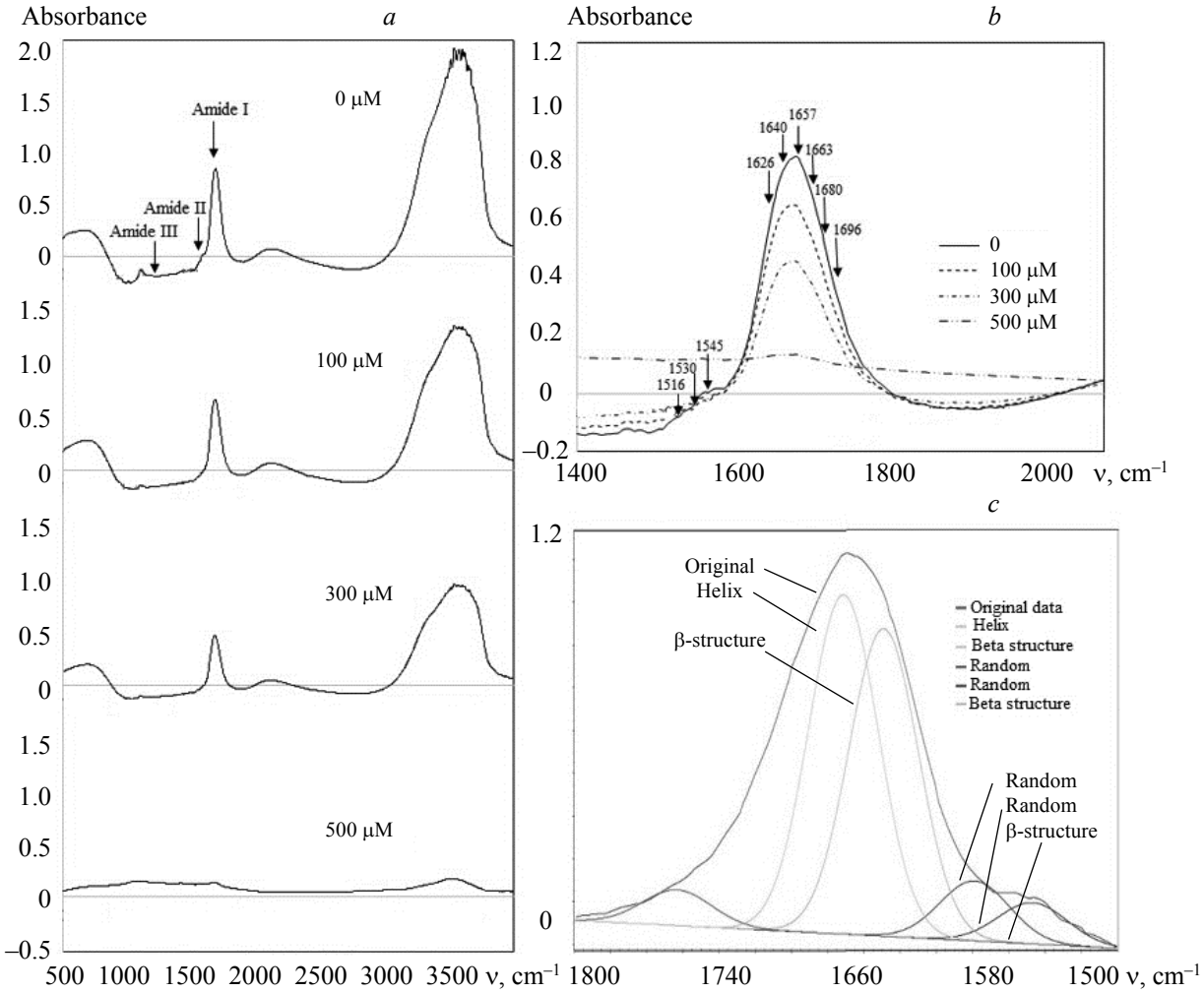

Fig. 3. FTIR spectrum of HRP solution. (a) FTIR spectrum of HRP in the presence of 0–500 μM Zn^{2+}. (b) Amide I and Amide II wavenumbers. (c) Amide I and Amide II bands deconvolute into a series of Gaussian contours.

The fluorescence quenching process in proteins results from the ground-state complex stability or non-fluorescent complex formation [22, 31] (Fig. 4). A Stern–Volmer plot was generated from a series of straight lines within the investigated Zn^{2+} concentration (Fig. 4b). K_{SV} and K_q were calculated by the linear fittings of the quenching experimental data. The results exhibited an excellent linear relationship within the investigated metal concentration, which indicated that the extinction process is linear and occurs uniformly as the Zn^{2+} concentration increases [32]. The fluorescence quenching in proteins occurs by static or dynamic mechanisms [33, 34]. According to previous studies, for dynamic quenching, the maximum K_q value of various quenchers is 2×10^{10} L/mole$^{-1}\cdot$ s^{-1} [35]. The results indicate that K_q is much higher than the criteria, which means that static quenching is responsible for the quenching process of HRP fluorescence by Zn^{2+}, which is caused by the formation of a complex between the enzyme and the Zn^{2+} rather than the dynamic collision. This result was confirmed by analyzing the modified Stern–Volmer plot and observing the existence of a reciprocal and linear relationship between $F_0/\Delta F$ and Zn^{2+} concentration ($[Q]^{-1}$). This result emphasizes that the mechanism of HRP quenching follows a static mechanism (Fig. 4c) [36]. These results are in accordance with earlier research on the interaction of cadmium with human serum albumin [37].

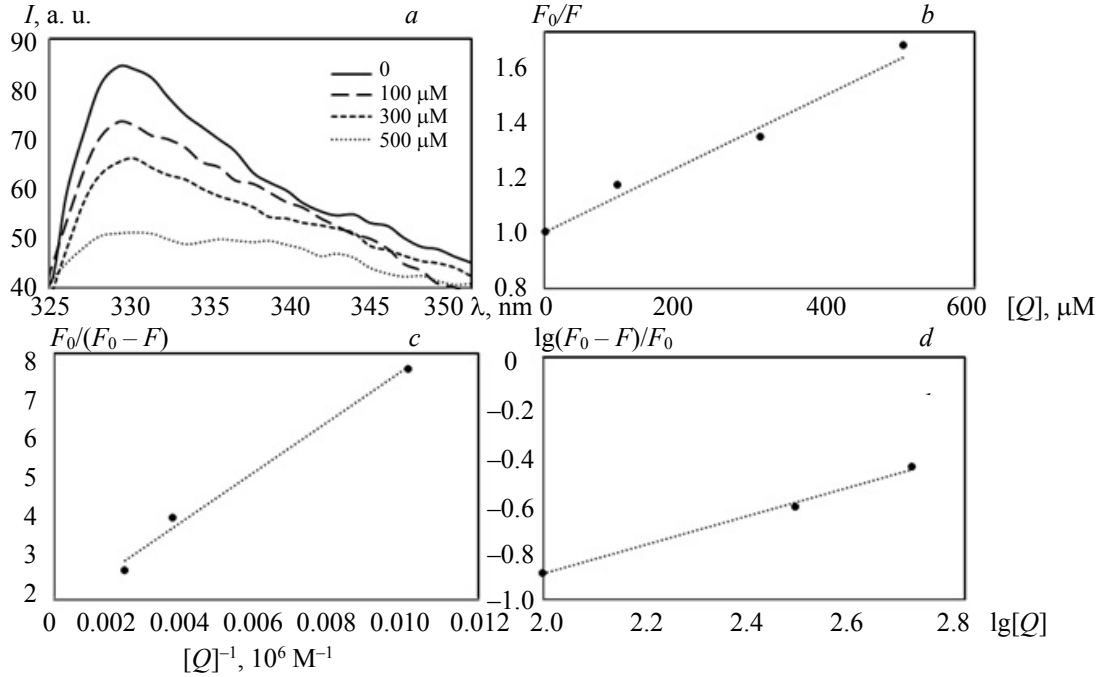

Fig. 4. Fluorescence spectroscopy plots of HRP–Zn^{2+} complex. (a) Tryptophan fluorescence emission spectra upon excitation at 295 nm for HRP in the presence of the different concentrations of Zn^{2+}. (b) Stern–Volmer plots of HRP quenching by 0–500 μM Zn^{2+}. (c) Modified Stern–Volmer plot for the binding of HRP–Zn^{2+}. (d) Plot of the dependence $\log(F_0–F/F_0)$ on $\log[Q]$ for the HRP–Zn^{2+} complex.

The other quenching parameters, *k*, and *n*, have been calculated from a modified Stern–Volmer plot for the binding of HRP–Zn^{2+} at 25ºC (Fig. 4d). As the number of binding sites equals approximately 1, there is a single class of binding sites with higher binding affinity and selectivity for Zn^{2+} to interact with HRP. HRP loses its secondary and tertiary structure compaction owing to the zinc metal treatment, whereas the enzyme structure compaction in the prosthetic group is increased. Under these conditions, the enzyme is more easily affected by temperature and, thus, reduces the temperature stability of the enzyme.

Conclusions. Previous studies indicated that zinc ions are a noncompetitive inhibitor for HRP and reduce the thermal stability and reactivation ability of HRP. In this investigation, the conformational changes responsible for HRP inhibition by Zn^{2+} were monitored by spectroscopic techniques. The results show that the α-helix and tertiary structure of HRP were reduced by Zn^{2+}. As the tryptophan residue is responsible for HRP fluorescence emission, the results can be attributed only to the areas around the tryptophan. Therefore, the quenching process is due to the formation of quencher bonds around the tryptophan of HRP through interactions with Zn^{2+}. Also, the microenvironment around the heme group did not change significantly. Moreover, Zn^{2+} interacts with a single class of binding sites on HRP through static quenching. The zinc ion is a heavy metal that frequently denatures HRP by reducing its structural elements and changing the microenvironment around tryptophan residue.

Acknowledgments. The authors would like to acknowledge the technical support provided by the Research Council of Islamic Azad University, Roudehen Branch, Roudehen, Iran.

REFERENCES

1. X. Zhao, J. Huang, J. Lu, Y. Sun, *Ecotoxic. Environ. Safety*, **170**, 218–226 (2019).
2. N. Bolan, A. Kunhikrishnan, R. Thangarajan, J. Kumpiene, J. Park, T. Makino, *J. Hazard Mater.*, **266**, 141–166 (2014).
3. J. Rahmani, Y. Fakhri, A. Shahsavani, Z. Bahmani, M. A. Urbina, S. Chirumbolo, H. Keramati, B. Moradi, A. Bay, G. Bjørklund, *Food Chem. Toxic.*, **118**, 753–765 (2018).
4. A. E. Belyaeva, N. L. Saris, *Biochem. Res. Int.*, 1–13 (2011).
5. F. Minibayeva, R. P. Beckett, I. Kranner, *Phytochemistry*, **112**, 122–129 (2015).

6. A. A. Khan, A. H. Rahmani, Y. H. Aldebasi, *Glob. J. Health Sci*., **6**, 87–98 (2014).
7. H. Nunavath, C. Banoth, V. R. Talluri, B. Bhukya, *Bioinformation*, **12**, 318–323 (2016).
8. V. Hooda, P. B. Gundala, P. Chinthala, *Bioinformation*, **8**, 974–979 (2012).
9. Y. Wang, Z. Ye, J. Li, Y. Zhang, Y. Guo, J. H. Cheng, *LWT*, **141**, 111078 (2021).
10. J. Sun, J. Zhao, L. Wang, H. Li, F. Yang, X. Yang, *ACS Sensors*, **3**, No. 1, 183–190 (2018).
11. S. Zhang, Z. Zheng, C. Zheng, Y. Zhao, Z. Jiang, *Food Chem*., **379**, 132142 (2022).
12. V. P. Pandey, M. Awasthi, S. Singh, S. Tiwari, U. N. Dwivedi, *Biochem. Anal. Biochem.*, **6**, 308–324 (2017).
13. K. V. S. K. Prasad, S. P. Paradha, P. Sharmila, *Environ. Exp. Bot*., **42**, 1–10 (1998).
14. G. I. Sat, *Afr. J. Biotech*., **7**, 2248–2253 (2008).
15. S. O. Malomo, R. I. Adeoye, L. Babatunde, I. A. Saheed, M. O. Iniaghe, F. J. Olorunniji, *Biochemistry*, **23**, No. 3, 1–5 (2019).
16. R. K. Behera, S. Goyal, S. Mazumdar, *J. Inorg. Biochem*., **104**, No. 11, 1185–1194 (2010).
17. L. Mao, S. Luo, Q. Huang, *Glycol. Sci. Rep*., **3**, 3126 (2013).
18. N. Hadizadeh Shirazi, *J. Food Biochem*., e12724 (**2018**).
19. N. Hadizadeh Shirazi, B. Ranjbar, K. H. Hajeh, Tohidi, *Int. J. Biol. Macromol*., **54**, 180–185 (2013).
20. K. Bamdad, B. Ranjbar, H. Naderi-Manesh, M. Sadeghi, *EXCLI J.*, **13**, 611–622 (2014).
21. H. Alsamamra, I. Khalid, R. Alfaqeh, M. Farroun, M. Abuteir, *J. Biomed. Sci*., **7**, 1–8 (2018).
22. V. D. Suryawanshi, L. S. Walekar, A. H. Gore, P. V. Anbhule, G. B. Kolekar, *J. Pharm. Anal*., **6**, 56–63 (2016).
23. C. L. Nnamchi, G. Parkin, I. Efimov, *J. Biol. Inorg. Chem*., **21**, 2163–2170 (2016).
24. R. A. Bozym, F. Chimienti, L. J. Giblin, G. W. Gross, I. Korichneva, Y. Li, S. Libert, W. Maret, M. Parviz, C. J. Frederickson, R. B. Thompson, *Exp. Biol. Med*., **235**, No. 6, 741–750 (2010).
25. S. Zhang, Z. Zheng, C. Zheng, Y. Zhao, Z. Jiang, *Food Chem*., **379**, 132–142 (2022).
26. M. S. Al-Bagmi, M. S. Khan, M. A. Ismael, A. M. Al-Senaidy, A. B. Bacha, F. M. Husain, S. F. Alamery, *Saudi J. Biol. Sci*., **26**, 301–307 (2019).
27. Z. Li, J. D. Hirst, *Chem. Sci*., **8**, 4318–4333 (2017).
28. A. J. Miles, R. W. Janes, B. A. Wallace, *Chem. Soc. Rev.* **50**, 8400–8413 (2021).
29. R. Arunkumar, C. J. Drummond, T. L. Greaves, *Front. Chem*., **7**, 74–79 (2019).
30. A. Sadat, I. J. Joye, *Appl. Sci*., **10**, No. 17, 5918–5925 (2020).
31. Z. Limpouchová, K. Procházka, In: *Fluorescence Studies of Polymer Containing Systems*, Ed. K. Procházka, Springer International Publishing, Cham, Swizerland, 91–149 (2016).
32. B. R. Masters, Book Review: Molecular Fluorescence, Principles and Applications (2013).
33. O. A. Plotnikova, A. G. Mel'nikov, G. V. Mel'nikov, *Opt. Spectrosc.*, **120**, 65–69 (2016).
34. K. Gao, R. Oerlemans, M. R. Groves, *Biophys. Rev*., **12**, No. 1, 85–104 (2020).
35. A. Papadopoulou, R. J. Green, R. A. Frazier, *J. Agric. Food Chem*., **53**, 158–163 (2005).
36. L. Zhao, R. Liu, X. Zhao, *Sci. Total Environ*., **407**, 5019–5023 (2009).
37. Y. Liu, M. Chen, L. Jiang, L. Song, *Environ. Sci. Poll. Res. Int*., **21**, 6994–7005 (2014).